



Cite this: *Chem. Commun.*, 2014, 50, 10251

Received 26th May 2014,
Accepted 15th July 2014

DOI: 10.1039/c4cc04020a

www.rsc.org/chemcomm

High performance asymmetrical push–pull small molecules end-capped with cyanophenyl for solution-processed solar cells†

Hang Gao,^a Yanqin Li,^a Lihui Wang,^a Changyan Ji,^a Yue Wang,^b Wenjing Tian,^b Xichuan Yang^a and Lunxiang Yin*^a

Two novel asymmetrical push–pull small molecules have been synthesized successfully, consisting of triphenylamine and diketopyrrolopyrrole as a fundamental dipolar D– π –A structure with ethynylbenzene as the π -bridge. TPATDPP end-capped with cyanophenyl exhibits a low optical band gap of 1.65 eV, and an impressive PCE of 5.94% has been achieved.

Solution-processed bulk heterojunction (BHJ) organic solar cells (OSCs) have experienced rapid development during the past two decades because they represent one of the most promising technologies for environmentally friendly solar energy conversion.¹ So far, fullerene derivatives such as PC₆₁BM and PC₇₁BM have been widely used as representative n-type acceptor materials for BHJ OSCs.² Much work has been done to develop novel p-type donors in order to maximize photovoltaic (PV) efficiency for commercialization. Small molecular donors (SMDs) have attracted considerable attention for preparing BHJ OSCs due to the advantages over their polymer counterparts, including well-defined molecular structures, easier purification and better batch-to-batch reproducibility.³ SMD-based BHJ single cells reported to date exhibit an encouraging power conversion efficiency (PCE) of 9.02%,⁴ which is comparable with the best PCE of 9.2% for polymers,⁵ making solution-processed SMD-based OSCs a fast growing field. However, the overall performance of SMD-based BHJ devices is still behind those of their polymer counterparts. Hence, solution-processed SMD-based OSCs still require better material design toward 10–15% efficiency for future applications.

To design ideal SMDs, alternating electron-donating (D) and electron-accepting (A) units in the conjugated backbone are commonly applied to improve PV performance,⁶ because such

architecture can not only easily reduce the energy band gap (E_g), but also effectively control the PV properties of materials. In general, the molecular configurations of most SMDs can be classified into two main categories: symmetrical D–A–D and A–D–A systems. In contrast, the solution-processed asymmetric dipolar D–A or D–A–A systems are relatively less explored, and their PV performance lags far behind those of symmetrical SMD-based OSCs.⁷ From the study of dye-sensitized solar cells, we learned that excellent organic dyes with D–A molecular architectures exhibited remarkably high PCEs of over 10%.⁸ In addition, important progress has been made on vacuum-deposited SMD-based OSCs with a PCE of 6.8%.⁹ Consequently, we believe that these asymmetrical push–pull small molecules possess attractive potential for BHJ OSCs. However, such types of molecules generally suffer from an insufficient light-absorption range, which may be one of the main impediments to further improvement of their performance.¹⁰ Therefore, it is highly desired to design new asymmetrical push–pull small molecules with narrow E_g for BHJ OSCs.

In this communication, two new asymmetrical push–pull small molecules **TPATDPP** and **TPATDPPCN** have been designed and synthesized, consisting of triphenylamine (TPA) and diketopyrrolopyrrole (DPP) as a fundamental dipolar D– π –A structure with ethynylbenzene as π -linkage, as shown in Fig. 1(a). In these molecules, the TPA unit behaves as the D building block due to its good hole-transporting capability and excellent

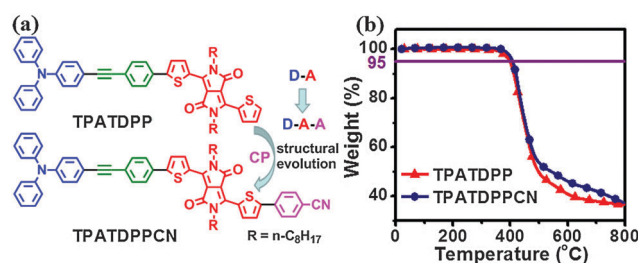


Fig. 1 Molecular structures (a) and TGA plots at a heating rate of 10 °C min⁻¹ under a nitrogen atmosphere (b) of **TPATDPP** and **TPATDPPCN**.

^a School of Chemistry, Dalian University of Technology, Dalian, China.
E-mail: lxyn@dlut.edu.cn; Fax: +86-411-84986040; Tel: +86-411-84986040

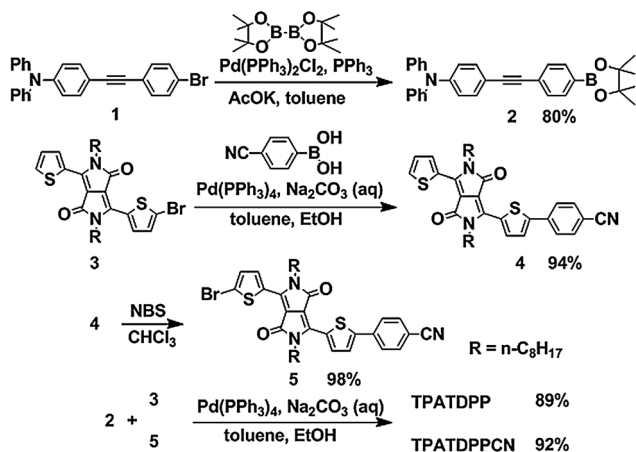
^b State Key Laboratory of Supramolecular Structure and Materials,
College of Chemistry, Jilin University, Changchun, China

† Electronic supplementary information (ESI) available: Measurement, characterization and calculation, synthesis and characterization, as well as PV device fabrication and hole-mobility measurement details. See DOI: 10.1039/c4cc04020a

electron-donating properties.¹¹ On the other hand, DPP has been regarded as a promising A group owing to its prominent electron-deficient properties and strong light-harvesting capacity, as well as excellent photochemical stability.¹² Moreover, ethynylbenzene-linkage could not only improve the molecular planarity but also facilitate the intramolecular charge transfer (ICT) process because of the coplanar and rigid nature of C≡C.¹³ In order to further extend the spectral regions, the cyano-group was introduced into the molecule as an A unit, which could effectively reduce E_g .¹⁴ Accordingly, an asymmetrical D–A–A-type TPATDPPCN end-capped with cyanophenyl (CP) was synthesized and studied, resulting in a low optical E_g of 1.65 eV in film. Finally, their PV properties were investigated using a simple spin-coating device. Among them, the TPATDPPCN-based device showed an impressive PCE of 5.94%, which is the highest efficiency reported to date for solution-processed D–A–A-type small molecule OSCs. The results indicate the great potential of such asymmetrical push–pull SMDs in creating high performance solution-processed OSCs.

The synthesis of TPATDPP and TPATDPPCN is described in Scheme 1. Starting from TPA, compound **1** was obtained by Pd-catalyzed Sonogashira reaction.^{11b,12c,15} By Miyaura borylation of compound **1** using Pd(PPh₃)₂Cl₂ as a catalyst, borate ester **2** was obtained in a yield of 80%. Compound **4** was prepared by Suzuki coupling of bromide **3** in a high yield of 94%. Bromide **5** was obtained by the NBS bromination of **4** under mild conditions with a high yield of 98%. Finally, TPATDPP and TPATDPPCN were facily synthesized by Pd-assisted Suzuki coupling in high yields of 89% and 92%, respectively. Detailed synthetic procedures and characterization are given in the ESI.† Their thermal stability was studied by thermogravimetric-analysis (TGA, see Fig. 1(b)). Their onset decomposition temperatures with 5% weight-loss are 397 °C and 408 °C, respectively, which demonstrate the exceptional thermal stability for their long-term PV applications.

The density functional theory (DFT) calculations were carried out to preliminarily investigate the influence of molecular structure on their electronic properties (the calculation method is given in the ESI†). The calculated energy levels and electronic-density



Scheme 1 Synthetic route for TPATDPP and TPATDPPCN.

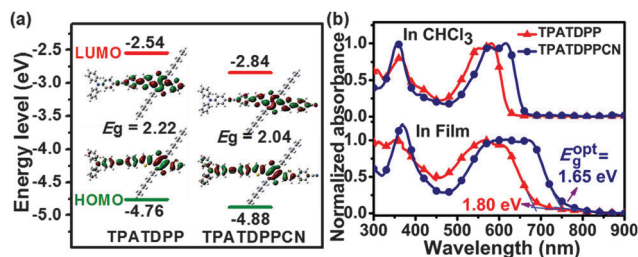


Fig. 2 (a) Theoretically calculated energy levels and electronic-density distribution; (b) normalized UV-vis absorption spectra of TPATDPP and TPATDPPCN in CHCl₃ and in thin film.

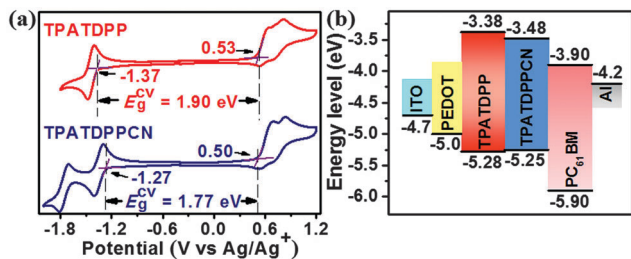
distribution are shown in Fig. 2(a). The electronic density of the highest occupied molecular orbital (HOMO) is distributed on the entire molecule whereas that of the lowest unoccupied molecular orbital (LUMO) is located on A units, showing an apparent ICT process existing in the push–pull molecules. In addition, both the HOMO and the LUMO of TPATDPPCN are lower than those of TPATDPP, which are attributed to the introduction of the CP unit. Moreover, the end-capped CP provoked a greater decrease of the LUMO, resulting in a large decrease of E_g from 2.22 eV of TPATDPP to 2.04 eV of TPATDPPCN.

The UV-vis absorption spectra of two SMDs in chloroform and in thin film are depicted in Fig. 2(b), and the corresponding optical data are summarized in Table 1. Both molecules exhibit a strong absorption in the long-wavelength region due to the ICT transition. It is worth mentioning that TPATDPPCN exhibits a higher molar extinction coefficient (ϵ) than that of TPATDPP (see Fig. S10 in ESI†). The solution of TPATDPP shows an absorption peak at 582 nm, and the spectrum of its film is broadened and red-shifted by 37 nm due to solid-state packing. In comparison with TPATDPP, spectra of TPATDPPCN both in solution and in film are greatly broadened and red-shifted to 614 and 671 nm, respectively, probably due to the stronger ICT transition and the stronger intermolecular interaction in the solid-state. As a result, the optical E_g of TPATDPP and TPATDPPCN corresponding to their absorption onsets is 1.80 eV and 1.65 eV, respectively.

The cyclic voltammogram (CV) measurements in dichloromethane were carried out to evaluate approximately the energy levels of the two molecules.^{12c,16} The CV curves are shown in Fig. 3(a), and the pertinent electrochemical data are summarized in Table 1 (experimental details and calculation are given in the ESI†). TPATDPP exhibits the onset reduction potential at -1.37 V, corresponding to the reduction of the DPP fragment. On the other hand, two reduction waves are observed in the cathodic potential regime for TPATDPPCN. The first onset reduction potential at -1.27 V can be ascribed to the reduction of the DPP fragment and the second one is assigned to the reduction of the CP group. In contrast to the reduction behavior, the oxidation potentials of the two molecules are relatively insensitive, and the first onset oxidation potentials are observed at 0.53 V and 0.50 V for TPATDPP and TPATDPPCN, respectively, corresponding to the oxidation of the TPA. As a result, the less-negative reduction potential and the slightly

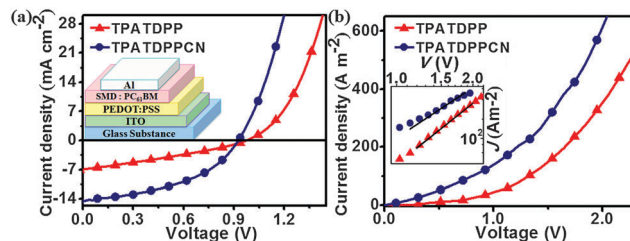
Table 1 Photophysical, electrochemical, hole mobility and PV performance data for **TPATDPP** and **TPATDPPCN**

| Compound | $\lambda_{\text{max}}^{\text{sol}}$ nm | $\lambda_{\text{max}}^{\text{film}}$ nm | E_g^{opt} eV | HOMO ^{CV} eV | LUMO ^{CV} eV | E_g^{CV} eV | μ_h $\text{cm}^2 \text{V}^{-1} \text{s}^{-1}$ | R_s Ωcm^2 | R_{sh} Ωcm^2 | V_{oc} V | J_{sc} mA cm^{-2} | FF | PCE (%) |
|------------------|---|--|--------------------------|--------------------------|--------------------------|-------------------------|--|-------------------------------|---|----------------------|--|------|------------|
| TPATDPP | 582 | 619 | 1.80 | -5.28 | -3.38 | 1.90 | 7.49×10^{-5} | 56.00 | 156 | 0.97 | 7.07 | 0.30 | 2.06 |
| TPATDPPCN | 614 | 671 | 1.65 | -5.25 | -3.48 | 1.77 | 1.51×10^{-4} | 11.40 | 251 | 0.93 | 14.86 | 0.43 | 5.94 |

Fig. 3 (a) CV curves of compounds in 0.1 M $\text{Bu}_4\text{NBF}_4/\text{CH}_2\text{Cl}_2$ at a scan rate of 100 mV s^{-1} ; (b) energy levels of the components for the PV device.

less-positive oxidation potential of **TPATDPPCN** relative to **TPATDPP** can be rationally ascribed to the presence of the electron-withdrawing CP block, resulting in a relatively low E_g of 1.77 eV. The energy level diagram of the components for the PV device is schematically depicted in Fig. 3(b). Both **TPATDPP** and **TPATDPPCN** in principle can behave as donors in BHJ OSCs, and the fairly low-lying HOMO would ensure a relatively large open-circuit voltage (V_{oc}). Notably, the narrow E_g of **TPATDPPCN** would result in an increased short-circuit current density (J_{sc}).

To investigate the PV properties of two SMDs, BHJ devices based on the SMDs:PC₆₁BM active layer with an area of 0.05 cm^2 were fabricated and characterized. The related current density–voltage (J – V) curves of the devices are described in Fig. 4(a) and the PV parameters are summarized in Table 1. The device based on **TPATDPP** with a lower HOMO level gave a relatively high V_{oc} of 0.97 V, a J_{sc} of 7.07 mA cm^{-2} , a fill factor (FF) of 0.30 and a PCE of 2.06%. Remarkably, the **TPATDPPCN** based device exhibits higher performance, with a V_{oc} of 0.93 V, a J_{sc} of 14.86 mA cm^{-2} , a FF of 0.43 and a PCE of 5.94%, in agreement with its higher photon-to-current response (see Fig. S11 in the ESI†). The high PV performance of the **TPATDPPCN**-based device can be attributed to both the narrow E_g induced by the CP group and the better carrier transporting capacity as evidenced by hole mobility (μ_h) measurements. Moreover, **TPATDPPCN** shows a stronger intermolecular interaction as evidenced by a more red-shifted absorption in film, contributing to its carrier transporting properties. Bear in mind that the charge mobility of the active layer might be closely related to the charge stability, and the film morphology as well as the intermolecular interaction. In order to investigate the μ_h of the synthesized SMDs, J – V characteristics of the hole-only devices were measured in the dark (details are given in the ESI†), as depicted in Fig. 4(b). By fitting the J – V curves in a double logarithmic scale to a space-charge-limited current (SCLC) model, as shown in the inset of Fig. 4(b), the μ_h can be derived. The μ_h values of **TPATDPP** and **TPATDPPCN** are 7.49×10^{-5} and $1.51 \times 10^{-4} \text{ cm}^2 \text{V}^{-1} \text{s}^{-1}$, respectively, and the data are summarized in Table 1. It is interesting to note that **TPATDPPCN**

Fig. 4 (a) J – V curves of BHJ devices with a configuration of ITO/PEDOT:PSS/SMDs:PC₆₁BM/Al under an illumination of AM 1.5 G at 100 mW cm^{-2} . Inset: device structure; (b) J – V curves of the hole-only devices with a structure of ITO/PEDOT:PSS/SMDs:PC₆₁BM/Au in the dark. Inset: the J – V curves in a double logarithmic scale and the solid lines are fits of the data points to a SCLC model.

exhibits about 2 times higher μ_h than that of **TPATDPP**, which is consistent with its high PV performance. Further experimental proof of better PV performance for **TPATDPPCN** is supported by its higher crystallinity (XRD patterns in Fig. S12, ESI†) and its better bicontinuous interpenetrating network (AFM images in Fig. S13, ESI†). In addition, the resistance changes are shown in Table 1. In contrast, the optimized D–A–A-typed **TPATDPPCN** reduces the series resistance (R_s) from $56 \Omega \text{ cm}^2$ to $11.40 \Omega \text{ cm}^2$ and increases the shunt resistance (R_{sh}) from $156 \Omega \text{ cm}^2$ to $251 \Omega \text{ cm}^2$, which leads to the increase of FF, J_{sc} and PCE. Further experiments on device optimization are underway in our laboratory.

In conclusion, two novel asymmetrical push–pull SMDs, **TPATDPP** and **TPATDPPCN**, have been synthesized and applied in the investigation of solution-processed BHJ OSCs. The dipolar D–A–A structural design end-capped with the CP unit enables **TPATDPPCN** to exhibit a narrow E_g , resulting in a high J_{sc} of 14.86 mA cm^{-2} with a high PCE of 5.94%. The efficiency is among the highest ever reported for solution-processed D–A–A-type small molecule-based BHJ OSCs. The high performance is primarily attributed to the narrow E_g and the reasonably low-lying HOMO level as well as the high hole-mobility. The results gave an important guide for developing novel asymmetrical push–pull small molecule PV materials.

This work was supported by the NSFC (No. 21102013, 51173065), the Dalian Committee of Science and Technology (2011J21DW001), the SRF for ROCS-SEM (No. 201001438, 201001439), the Fundamental Funds for the Central Universities (DUT11LK20) and the RFDP (No. 20090041120017).

Notes and references

- (a) A. J. Heeger, *Adv. Mater.*, 2014, **26**, 10; (b) F. Liu, Y. Gu, X. Shen, S. Ferdous, H.-W. Wang and T. P. Russell, *Prog. Polym. Sci.*, 2013, **38**, 1990; (c) J.-M. Jiang, M.-C. Yuan, K. Dinakaran, A. Hariharan and K.-H. Wei, *J. Mater. Chem. A*, 2013, **1**, 4415.

- 2 (a) C.-Z. Li, H.-L. Yip and A. K.-Y. Jen, *J. Mater. Chem.*, 2012, **22**, 4161; (b) Y. Kim and E. Lim, *Polymers*, 2014, **6**, 382.
- 3 (a) J. Roncali, P. Leriche and P. Blanchard, *Adv. Mater.*, 2014, **26**, 3821; (b) Y. Lin, Y. Li and X. Zhan, *Chem. Soc. Rev.*, 2012, **41**, 4245; (c) A. Mishra and P. Bäuerle, *Angew. Chem., Int. Ed.*, 2012, **51**, 2020; (d) Y. Chen, X. Wan and G. Long, *Acc. Chem. Res.*, 2013, **46**, 2645; (e) Y. Liu, C.-C. Chen, Z. Hong, J. Gao, Y. Yang, H. Zhou, L. Dou, G. Li and Y. Yang, *Sci. Rep.*, 2013, **3**, 3356, DOI: 10.1038/srep03356.
- 4 V. Gupta, A. K. K. Kyaw, D. H. Wang, S. Chand, G. C. Bazan and A. J. Heeger, *Sci. Rep.*, 2013, **3**, 1965, DOI: 10.1038/srep01965.
- 5 Z. He, C. Zhong, S. Su, M. Xu, H. Wu and Y. Cao, *Nat. Photonics*, 2012, **6**, 591.
- 6 (a) H. Zhou, L. Yang and W. You, *Macromolecules*, 2012, **45**, 607; (b) J. E. Coughlin, Z. B. Henson, G. C. Welch and G. C. Bazan, *Acc. Chem. Res.*, 2014, **47**, 257; (c) Y. Li, Q. Guo, Z. Li, J. Pei and W. Tian, *Energy Environ. Sci.*, 2010, **3**, 1427.
- 7 (a) S. Paek, N. Cho, K. Song, M.-J. Jun, J. K. Lee and J. Ko, *J. Phys. Chem. C*, 2012, **116**, 23205; (b) H. Bürckstümmer, E. V. Tulyakova, M. Deppisch, M. R. Lenze, N. M. Kronenberg, M. Gsänger, M. Stolte, K. Meerholz and F. Würthner, *Angew. Chem., Int. Ed.*, 2011, **50**, 11628; (c) W. Zhang, S. C. Tse, J. Lu, Y. Tao and M. S. Wong, *J. Mater. Chem.*, 2010, **20**, 2182.
- 8 (a) S. Ahmad, E. Guillén, L. Kavan, M. Grätzel and M. K. Nazeeruddin, *Energy Environ. Sci.*, 2013, **6**, 3439; (b) H. N. Tsao, J. Burschka, C. Yi, F. Kessler, M. K. Nazeeruddin and M. Grätzel, *Energy Environ. Sci.*, 2011, **4**, 4921.
- 9 Y.-H. Chen, L.-Y. Lin, C.-W. Lu, F. Lin, Z.-Y. Huang, H.-W. Lin, P.-H. Wang, Y.-H. Liu, K.-T. Wong, J. Wen, D. J. Miller and S. B. Darling, *J. Am. Chem. Soc.*, 2012, **134**, 13616.
- 10 L.-Y. Lin, Y.-H. Chen, Z.-Y. Huang, H.-W. Lin, S.-H. Chou, F. Lin, C.-W. Chen, Y.-H. Liu and K.-T. Wong, *J. Am. Chem. Soc.*, 2011, **133**, 15822.
- 11 (a) S. Zeng, L. Yin, C. Ji, X. Jiang, K. Li, Y. Li and Y. Wang, *Chem. Commun.*, 2012, **48**, 10627; (b) L. Wang, L. Yin, C. Ji, Y. Zhang, H. Gao and Y. Li, *Org. Electron.*, 2014, **15**, 1138.
- 12 (a) S. Qu and H. Tian, *Chem. Commun.*, 2012, **48**, 3039; (b) L. Zhang, S. Zeng, L. Yin, C. Ji, K. Li, Y. Li and Y. Wang, *New J. Chem.*, 2013, **37**, 632; (c) C. Ji, L. Yin, L. Wang, T. Jia, S. Meng, Y. Sun and Y. Li, *J. Mater. Chem. C*, 2014, **2**, 4019.
- 13 (a) X. Zhao, L. Ma, L. Zhang, Y. Wen, J. Chen, Z. Shuai, Y. Liu and X. Zhan, *Macromolecules*, 2013, **46**, 2152; (b) W. A. Braunecker, S. D. Oosterhout, Z. R. Owczarczyk, R. E. Larsen, B. W. Larson, D. S. Ginley, O. V. Boltalina, S. H. Strauss, N. Kopidakis and D. C. Olson, *Macromolecules*, 2013, **46**, 3367.
- 14 X. Liu, M. Li, R. He and W. Shen, *Phys. Chem. Chem. Phys.*, 2014, **16**, 311.
- 15 J.-K. Fang, D.-L. An, K. Wakamatsu, T. Ishikawa, T. Iwanaga, S. Toyota, D. Matsuo, A. Orita and J. Otera, *Tetrahedron Lett.*, 2010, **51**, 917.
- 16 (a) J.-L. Bredas, *Mater. Horiz.*, 2014, **1**, 17; (b) A. Yassin, P. Leriche, M. Allain and J. Roncali, *New J. Chem.*, 2013, **37**, 502; (c) X. Liu, Y. Sun, B. B. Y. Hsu, A. Lorbach, L. Qi, A. J. Heeger and G. C. Bazan, *J. Am. Chem. Soc.*, 2014, **136**, 5697.